IAI Journals.ASM.org

The Sphingosine-1-Phosphate Analogue FTY720 Impairs Mucosal Immunity and Clearance of the Enteric Pathogen *Citrobacter rodentium*

Carola T. Murphy, Lindsay J. Hall,* Grainne Hurley, Aoife Quinlan, John MacSharry, Fergus Shanahan, Kenneth Nally, and Silvia Melgar

Alimentary Pharmabiotic Centre, University College Cork, National University of Ireland, Cork, Ireland

The sphingosine-1-phosphate (S1P) analogue FTY720 is therapeutically efficacious in multiple sclerosis and in the prevention of transplant rejection. It prevents the migration of lymphocytes to sites of pathology by trapping them within the peripheral lymph nodes, mesenteric lymph nodes (MLNs), and Peyer's patches. However, evidence suggests that its clinical use may increase the risk of mucosal infections. We investigated the impact of FTY720 treatment on susceptibility to gastrointestinal infection with the mouse enteric pathogen *Citrobacter rodentium*. This attaching and effacing bacterium induces a transient bacterial colitis in immunocompetent mice that resembles human infection with pathogenic *Escherichia coli*. FTY720 treatment induced peripheral blood lymphopenia, trapped lymphocytes in the MLNs, and prevented the clearance of bacteria when mice were infected with luciferase-tagged *C. rodentium*. FTY720-treated *C. rodentium*-infected mice had enhanced colonic inflammation, with significantly higher colon mass, colon histopathology, and neutrophil infiltration than vehicle-infected animals. In addition, FTY720-treated infected mice had significantly lower numbers of colonic dendritic cells, macrophages, and T cells. Gene expression analysis demonstrated that FTY720-treated infected mice had an impaired innate immune response and a blunted mucosal adaptive immune response, including Th1 cytokines. The data demonstrate that the S1P analogue FTY720 adversely affects the immune response to and clearance of *C. rodentium*.

Therapeutic use of the sphingosine-1-phosphate (S1P) analogue FTY720 (fingolimod [trade name, Gilenya]) has proven efficacy in patients with multiple sclerosis (MS) and was recently approved by the U.S. Food and Drug Administration as a first-line treatment for relapsing forms of the disease (1, 27). FTY720 modulates S1P signaling, preventing lymphocyte egress from the thymus and spleen into the blood and from the lymph nodes (LNs) into the lymph, thus blocking lymphocyte trafficking to target tissues (5, 6). It also affects dendritic cell (DC) migration (16, 31), modulates DC proinflammatory signaling, and is a potent inhibitor of regulatory T cell (Treg) proliferation (56). Controversy surrounds the complex mechanism of action of FTY720 *in vivo*, and it is unclear whether it acts as an agonist, a functional antagonist, or both during the regulation of lymphocyte recirculation (21, 47, 52, 58). FTY720 ameliorated disease in numerous preclinical models of colitis, including those induced by oxazolone (12), 2,4,6-trinitrobenzene sulfonic acid (11), dextran sulfate sodium (14), and adoptive transfer (14, 18), and in interleukin-10 (IL-10)-deficient mice (36). In addition, it was therapeutically efficacious in graft-versus-host disease (24) and in studies of transplantation and MS (2, 4, 23). However, treatment with FTY720 may increase the risk of mucosal infections and its effect on host immune responses upon exposure to such threats has yet to be completely elucidated. Two fatal herpesvirus infections were reported in a phase 3 clinical study comparing FTY720 with beta interferon (IFN-β) (7, 19), and an increased incidence of respiratory tract infections, such as bronchitis, have been reported in MS patients undergoing FTY720 treatment (8, 28). Nonetheless, studies to date that have assessed the effect of FTY720 on innate and adaptive immune responses have specifically focused on exposure to viral antigens and vaccines (30, 35). There are no studies that have examined the effect of FTY720 treatment following exposure to gastrointestinal infections.

In the present study, we assessed the effect of continuous dosing of FTY720 on the susceptibility of mice to *Citrobacter rodentium*, a commonly used noninvasive enteropathogen that is a model for human enteropathogenic and enterohemorrhagic *Escherichia coli* infections. *C. rodentium* intimately attaches to the apical surface of the gut epithelium, inducing epithelial cell actin rearrangements and localized destruction of brush border microvilli and leading to the formation of underlying pedestal-like attaching and effacing lesions in the host cell (29). Oral infection of immunocompetent mice with *C. rodentium* leads to a transient colonization and inflammation that peaks after 1 week and is cleared in the ensuing 2 to 3 weeks (37). Bacterial colonization is limited to the intestinal mucosa, with light bacterial burdens in systemic organs. The mice exhibit mild signs of clinical disease, and microscopically, the mucosa presents crypt hyperplasia, goblet cell loss, and mucosal infiltration of immune cells, including T

Received 14 December 2011 **Returned for modification** 17 January 2012
Accepted 14 May 2012

Published ahead of print 21 May 2012

Editor: B. A. McCormick

Address correspondence to Silvia Melgar, s.melgar@ucc.ie.

* Present address: Lindsay J. Hall, Institute of Food Research, Norwich Research Park, Colney, Norwich, United Kingdom.

S.M. and K.N. share joint senior authorship of this work.

Supplemental material for this article may be found at http://iai.asm.org/.

Copyright © 2012, American Society for Microbiology. All Rights Reserved.

doi:10.1128/IAI.06319-11

cells, macrophages, and neutrophils. For efficient bacterial clearance, a robust Th1 host immune response is required, mediated by infiltrating $CD4^+$ T cells and macrophages. Thus, *C. rodentium* infection is an excellent model for the investigation of host-bacterium immune interactions in the intestine. In addition, the availability of a bioluminescent strain that allows pathogen burden and clearance dynamics to be monitored *in vivo* by bioluminescence imaging makes this model a versatile tool (9, 17, 40). Our data clearly show that continuous treatment with FTY720 delays the clearance of *C. rodentium* infection in mice by blocking the migration of T cells and other immune cells to the inflamed colon. Host protective mucosal immunity is altered with impairment of innate and adaptive immune responses. This is the first report, to our knowledge, that FTY720 can compromise the critical host defense against commonly encountered enteric pathogens.

MATERIALS AND METHODS

Mice. Specific-pathogen-free female C57BL/6OlaHsD mice, 7 to 12 weeks old and weighing 17 to 20 g, were obtained from Harlan UK. All mice were housed in individually ventilated cages (OptiMICE; Animal Care Systems) in groups of 3 or 4 mice per cage with sterile bedding, a temperature of 21°C, 12 h light and 12 h darkness, and 50% humidity in a dedicated animal holding facility. They were fed a sterilized pellet diet and tap water *ad libitum*. Mice were allowed ≥2 weeks to acclimatize before entering the study. All animal procedures were performed according to national ethical guidelines following approval by the University College Cork Animal Experimentation Ethics Committee.

***C. rodentium*-induced colitis.** Bioluminescent *C. rodentium* strain ICC180 was a gift from Gordon Dougan (Wellcome Trust Sanger Institute). This nalidixic acid (NA)-resistant strain harbors a constitutively expressed luminescent tag that enables the colonization pattern to be monitored by bioluminescence imaging. Previous studies have shown a strong correlation between cell numbers and bioluminescent signals (15, 43). Similarly, levels of light emitted by bioluminescent *C. rodentium* strains have been shown to accurately reflect bacterial numbers *in vivo* (55). *C. rodentium* strain ICC180 was cultured overnight in Luria-Bertani (LB) broth supplemented with NA (50 μg/ml; Sigma-Aldrich Ltd., Dublin, Ireland) at 37°C, centrifuged at 3,000 × *g* for 10 min, and resuspended in 10 ml of sterile phosphate-buffered saline (PBS) for oral gavage. Each mouse received 200 μl (approximately 5×10^9 bacteria) of the bacterial suspension. Postgavage, the remainder of the suspension was plated in serial dilutions for retrospective enumeration. For bacterial enumeration in stool samples collected at different time points, serial dilutions of a fecal-PBS suspension (ranging from undiluted to 10^{-7} dilution) were plated on supplemented LB agar by a spot plate technique and incubated overnight at 37°C. To determine the number of bacteria in the spleen, the organ was weighed, manually crushed in 2 ml of PBS in a stomacher bag, plated using serial dilutions onto supplemented LB agar, and incubated overnight at 37°C.

FTY720 administration. To assess the effect of continuous dosing of FTY720 on *C. rodentium*-induced colitis, mice were orally gavaged with the vehicle (1% methylcellulose; Sigma-Aldrich Ltd., Dorset, England) or 3 mg/kg FTY720 for 6 days preinfection (day −6 to day −1 inclusive). Mice were orally gavaged with *C. rodentium* on day 0, and vehicle or FTY720 dosing was continued every second day from day 1 until day 12 postinfection (p.i.). Mice were sacrificed at two time points, on day 8 (peak infection) and on day 14 (late infection/clearance). The number of mice per group per time point was 7. Noninfected controls were dosed with the vehicle or FTY720 according to the same regimen ($n = 4$ per group). The compound FTY720 was kindly provided by A. Haynes (GlaxoSmithKline, Stevenage, United Kingdom).

In a separate study, we investigated the effect of stopping FTY720 dosing early during *C. rodentium* infection. In this instance, as with the continuous-dosing study, the mice were orally gavaged daily with the vehicle (1% methylcellulose) or 3 mg/kg FTY720 for 6 days preinfection (day −6 to day −1 inclusive). Following infection on day 0, dosing was continued for only 2 days. Mice were sacrificed on day 14. The number of mice per group was 7.

Clinical assessment of inflammation. Body weight was monitored regularly. Clinical assessment of inflammation was adapted from other colitis models (38, 39). Briefly, stool consistency (0, normal, well-formed pellets; 1, changed formed pellets; 2, loose stool; 3, diarrhea) and fur texture/posture (0, smooth coat/not hunched; 1, mildly scruffy/mildly hunched; 2, very scruffy/very hunched) were recorded every second day for the duration of the study to generate a disease activity index.

***In vivo* bioluminescence imaging.** On days 8 and 14 p.i., *in vivo* bioluminescence imaging was performed as previously described (10, 51), with an IVIS 100 charge-coupled device imaging system (Xenogen, Alameda, CA). Briefly, following anesthetization with 3% isoflurane gas, the animals were transferred to the imaging chamber, where emission images were collected with 5-min integration times. Following whole-body imaging, the mice were euthanized via cardiac puncture. The colons were removed, detached from the ceca, cut longitudinally, washed in PBS, and imaged for 5 min. The ceca were also washed in PBS prior to imaging. The mesenteric LNs (MLNs) and spleens were removed and imaged. Bioluminescent signals were quantified by the creation of regions of interest (ROIs). To standardize the data, light emission from the same surface area (ROI) was quantified for each organ type. In addition, background light emission, taken from ROIs created on organs of noninfected control animals, was subtracted from test organs. Imaging data were analyzed and quantified with Living Image Software (Xenogen) and expressed as photons/second/cm^2.

Histology. The colons were removed, opened longitudinally, washed in PBS, and separated into proximal and distal sections. The length of each colon was measured, and 3 cm was taken as the distal end. The proximal and distal colons were weighed and cut longitudinally, and one section of the distal end was processed as a "Swiss roll" and snap-frozen in optimal cutting temperature compound (Tissue-Tek; Sakura Finetek) using liquid nitrogen. Frozen colons were cryosectioned (6 μm), fixed for 5 min in ice-cold acetone-ethanol (3:1 ratio), and stained with hematoxylin and eosin according to standard histological procedures. Colon sections were evaluated and assigned scores in a blinded fashion for evidence of inflammatory damage such as goblet cell loss, crypt elongation, mucosal thickening, and epithelial injury, including hyperplasia and enterocyte shedding into the gut lumen. Scores were determined for four fields of view per mouse at ×20 magnification (Olympus BX51) on a scale of 0 to 3 (0, none; 1, mild; 2, moderate; 3, severe). A mean inflammatory score was then assigned per mouse distal colon, $n = 3$ or 4 mice per group.

Immunofluorescent staining. Frozen colon and MLN sections (6 μm) were fixed in an ice-cold acetone-alcohol mixture (3:1 ratio), blocked with blocking serum for 45 min at room temperature in a humidified chamber, and stained with combinations of the monoclonal antibodies (MAbs) listed in Table 1. Purified MAbs were counterstained using the appropriate Alexa Fluor 488-conjugated anti-Ig antibody (Invitrogen, Biosciences Ltd.). Hoechst (Invitrogen) was used as a nuclear counterstain. Stained sections were mounted in ProLong Gold antifade reagent (Invitrogen), coded, and visualized using a fluorescence microscope (Olympus BX51) in a blinded fashion. For cell number quantitation, 7 to 10 fields of view were counted at a magnification of ×40 for 3 or 4 mice per group.

Flow cytometry. Blood was harvested from the mice via cardiac puncture on days 8 and 14 into 0.01 M EDTA (Sigma-Aldrich) and lysed in 2 ml ACK (buffered ammonium chloride) lysis buffer (0.15 M NH_4Cl, 1 mM $KHCO_3$, 0.1 mM EDTA, pH 7.2). Following centrifugation, the red layer was removed, leaving the clear pellet containing the white blood cells. A final concentration of 2×10^5 cells/well was resuspended in blocking buffer. To this cell suspension, 50 μl of each MAb-dye mixture was added and it was incubated in the dark at 4°C for 30 min. Combinations of the MAbs listed in Table 1 were used in this study. Following staining, the cells

TABLE 1 Antibodies used in this study

Target molecule	Host	Clone	Isotype	Conjugate[a]	Source
CD3	Hamster	145-2C11	IgG1	APC	BD Biosciences
CD3	Hamster	145-2C11	IgG	PE	BioLegend
CD11c	Hamster	HL3	IgG1	PE	BD Biosciences
Ly6G	Rat	1A8	IgG2a	PE	BioLegend
CD19	Rat	6D5	IgG2a	None	BioLegend
B220	Rat	RA3-6B2	IgG2a	Alexa Fluor 700	AbD Serotec
F4/80	Rat	CI:A3-1	IgG2b	None	Abcam
F4/80	Rat	BM8	IgG2b	TRI-COLOR	Caltag
NK1.1	Mouse	PK136	IgG2a	PerCp-CY5.5l	BioLegend
Rat IgG	Goat		IgG	Alexa Fluor 488	Invitrogen
Rabbit IgG	Goat		IgG	Alexa Fluor 488	Invitrogen

[a] APC, allophycocyanin; PE, phycoerythrin; PerCp, peridinin chlorophyll protein.

were washed twice with blocking buffer and fixed in 1% paraformaldehyde. Relative fluorescence intensities were measured using an LSRII cytometer and BD Diva software. For each sample, 10,000 to 20,000 events were recorded. The percentage of cells labeled with each MAb was calculated in comparison with cells stained with isotype control antibody. Analysis gates for each antibody were set by using FMO (fluorescence minus one) controls with a threshold below 1%. The results represent the percentage of positively stained cells in the total cell population exceeding the background staining signal.

RNA extraction and qPCR. Colonic mucosal mRNA expression was evaluated using real-time quantitative PCR (qPCR). The distal colons were weighed and cut longitudinally, and one section was snap-frozen in 1 ml RNAlater. Frozen colonic tissue samples were thawed on ice and transferred to MagNA Lyser tubes with green beads (Roche Ireland Limited, Clare, Ireland) containing 1 ml of lysis buffer (provided with the mirVana kit; Ambion, Applied Biosystems). Samples were homogenized three times for 15 s each time at 6,500 × *g* using a MagNA Lyser instrument (Roche). Homogenized samples were centrifuged at 200 × *g* for 5 min at 4°C, and the supernatants were stored at −80°C. Total RNA was isolated from colonic tissue homogenates by using the mirVana kit according to the manufacturer's protocol. RNA purity was measured by spectrophotometric analysis using a NanoDrop. cDNA was synthesized using 1 μg total RNA. PCR primers and probes were designed using the Universal ProbeLibrary Assay Design Centre (http://www.roche-applied-science.com/sis/rtpcr/upl/index.jsp). Assays were designed for murine IL-1β, IL-12p40, IL-6, IL-4, IL-10, IL-17a, IL-22, IL-23a, NOS2 (inducible nitric oxide synthase [iNOS]), IFN-γ, Rorc (retinoic acid-related orphan receptor gamma t [RORγt]), Tbx21 (Tbet), tumor necrosis factor alpha (TNF-α), Foxp3, and RegIIIγ. Primer sequences and corresponding probe numbers are available upon request. The gene for β-actin was used as a housekeeping gene to correct for variability in the initial amount of total RNA. All PCRs were performed in triplicate using 384-well plates on the LightCycler 480 System (Roche). Positive and negative controls were also included. The $2^{-\Delta\Delta CT}$ method (33) was used to calculate relative changes in gene expression determined from qPCR experiments.

Statistical analysis. Data are presented as the mean ± the standard error of the mean (SEM) unless otherwise stated. The specific tests used are indicated in the figure legends. All statistical tests were performed using commercially available statistical software (GraphPad Software Inc.). A P value of <0.05 was considered significant.

RESULTS

FTY720 induces peripheral blood lymphopenia by trapping lymphocytes within LNs. The effect of FTY720 on immune cell populations in the blood of *C. rodentium*-infected mice was assessed at various time points during the treatment period by flow cytometry. A significant reduction of the T cell count in the blood (lymphopenia) was observed in the FTY720-treated animals, compared to those that received the vehicle on days 8 and 14 p.i. (Fig. 1A), in accordance with previous reports (35). A similar reduction of the levels of B cells was observed on day 8, but not on day 14, p.i. (Fig. 1A). Additionally, a significant increase in DCs was observed in the blood of the FTY720-treated mice on day 14 p.i., but not on day 8 p.i. (Fig. 1A). FTY720 treatment appeared to have no effect on levels of granulocytes (Fig. 1A), monocytes, NK cells, or NKT cells in blood (data not shown) at either of the time points analyzed. Noninfected controls treated with the same vehicle or FTY720 dosing regimen showed similar results on day 14 (see Fig. S1A in the supplemental material).

Immunofluorescent staining of frozen tissue sections demonstrated a marked accumulation of $CD3^+$ T cells in the MLNs of FTY720-treated mice on day 14 p.i., confirming the inhibitory effect of the S1P analogue on their egress from secondary lymphoid organs (Fig. 1B).

FTY720 treatment increases the pathogen burden and impairs bacterial clearance. To determine the effects of FTY720 on *C. rodentium* infection in mice, we visualized and quantitated the levels and tissue distribution of the pathogen on days 8 and 14 p.i. by using bioluminescence imaging. Whole-body imaging revealed a large pathogen burden in the lower abdominal/gastrointestinal region of both the vehicle-treated and FTY720-treated mice at day 8 p.i. (Fig. 2A). However, the bioluminescent signal from the FTY720-treated animals was significantly greater ($P < 0.001$, Fig. 2A and C). At day 14 p.i., while whole-body imaging revealed clearance of the bacteria by the infected, vehicle-treated mice, as evidenced by a significantly diminished bioluminescent signal, no such clearance was evident in the infected, FTY720-treated mice (Fig. 2B and C). *Ex vivo* bioluminescence imaging of the organs at day 8 p.i. revealed significantly greater colonization of the ceca ($P < 0.05$), colons ($P < 0.05$), spleens ($P < 0.01$), and MLNs ($P < 0.001$) of the FTY720-treated mice than those of the vehicle-treated mice (Fig. 2D). *C. rodentium* initially infects the cecum and then moves onto the distal colon. We and others have confirmed this colonization pattern by using bioluminescence (55). In the present study, 100% of the FTY720-treated mice had evidence of bacteria in the cecum on day 8 p.i., compared to 28% of those that received the vehicle. By day 14 p.i., in contrast to the vehicle-treated mice, the signal from the colons and ceca remained high in the FTY720-treated animals and there was evidence of MLN infection in just under half of the mice (Fig. 2D). The bioluminescence data were supported by fecal CFU counts, which were performed at various time points p.i. These confirmed that day 8 was

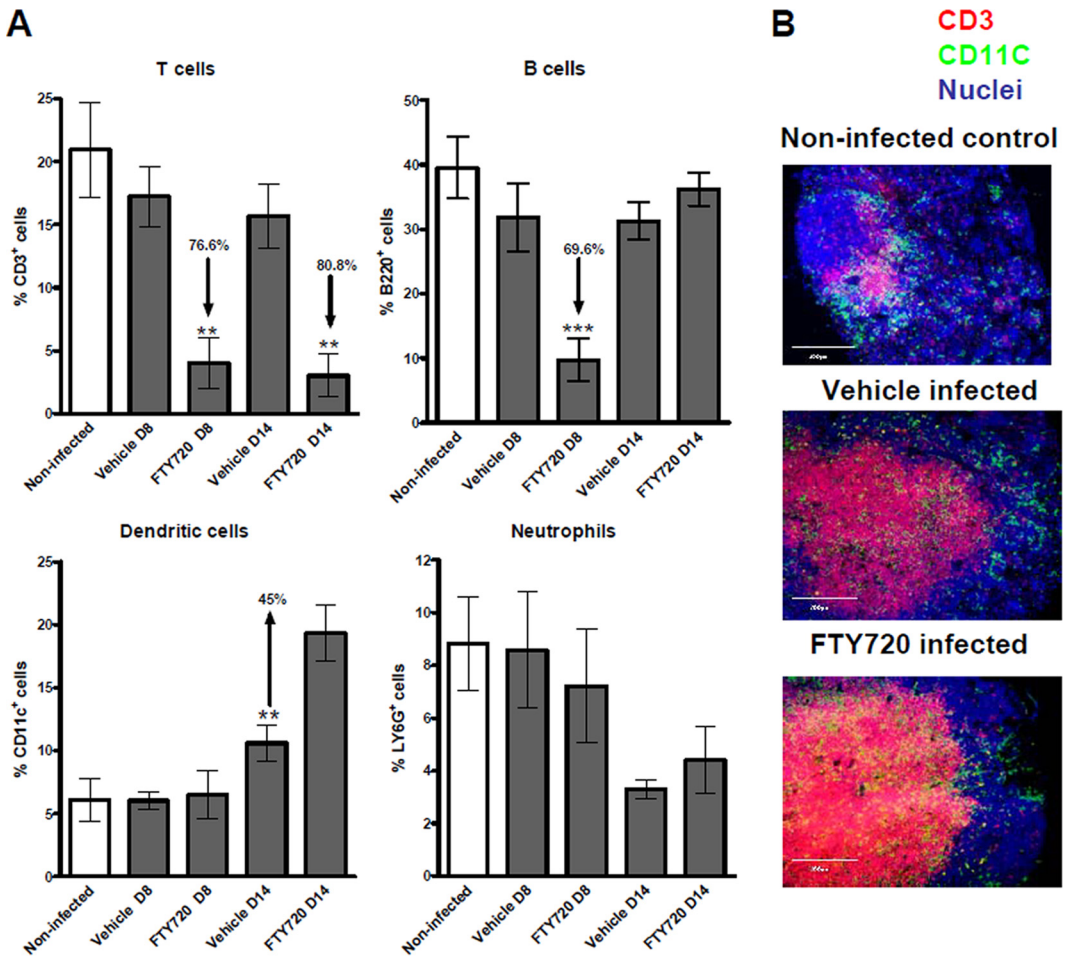

FIG 1 FTY720 induces peripheral blood lymphopenia by trapping T cells in MLNs. (A) Leukocytes were isolated from the blood of noninfected and *C. rodentium*-infected animals on day 8 (D8; peak infection) and day 14 (D14; clearance) p.i. and stained with fluorochrome-labeled MAb. They were analyzed by flow cytometry, in which 10,000 to 20,000 events were recorded. The data represent the mean percentages of $CD3^+$ (T cells), $B220^+$ (B cells), $CD11c^+$ (DCs), and $Ly6G^+$ cells (neutrophils). The significance of differences from vehicle-treated controls was determined by one-way analysis of variance, followed by Bonferroni's multiple-comparison test (***, $P < 0.001$; **, $P < 0.01$; *, $P < 0.05$; $n = 4$ to 7 individual mice). (B) FTY720 traps T cells and DCs within the MLNs. Shown is an *in situ* visualization of leukocytes within the MLNs of noninfected and *C. rodentium*-infected vehicle-treated and FTY720-treated animals on day 14 p.i. Tissue sections from 4 individual mice per group were analyzed by fluorescence microscopy. Frozen MLN sections (6 μm) were fixed in acetone-ethanol, stained for $CD11c^+$ cells (green), and costained for $CD3^+$ cells (red) and nuclei (blue). A representative picture for each group is shown. (Original magnification, ×20). Scale bars, 200 μm.

close to peak infection (Fig. 2E). In addition, FTY720-treated mice shed significantly higher numbers of *C. rodentium* bacteria in their stool from day 9 p.i. on than vehicle-treated controls and showed no signs of clearing the infection. Bacterial numbers in the feces of the drug-treated animals continued to increase over time (Fig. 2E), while those of the vehicle-treated animals began to drop after day 7 p.i. Splenic bacterial counts were similar between vehicle-treated and FTY720-treated animals on day 8 p.i. However, on day 14 p.i., the vehicle-treated animals no longer had any evidence of bacterial growth in this organ, while the bacterial burdens in the spleens of mice that received the S1P analogue remained large (Fig. 2F). In contrast to the vehicle-treated mice, FTY720-treated animals did not resolve the infection by day 14 p.i. and still had high concentrations of bacteria in all of the organs analyzed.

FTY720 treatment exacerbates clinical and colonic pathology during *C. rodentium* infection. To determine the effect of FTY720 administration on disease during *C. rodentium* infection, we monitored clinical and macroscopic signs of inflammation postinfection. In all of the mice infected with *C. rodentium*, weight loss was absent or minimal (see Fig. S2A in the supplemental material) and the disease activity scores were well below the maximum possible, i.e., 5 on the scale used (mean, 0.4 at day 8 p.i. and 0.9 on day 14 p.i. in the vehicle-treated mice; see Fig. S2B in the supplemental material). Nevertheless, there was a significant increase in the disease activity scores of FTY720-treated mice on days 7 ($P < 0.01$), 8 ($P < 0.01$), and 10 ($P < 0.05$) p.i., respectively, compared to those of vehicle-treated mice (see Fig. S2B in the supplemental material). These time points are considered to represent peak infection with the bacteria. No differences in colon length were evident between the vehicle-treated (5.8 ± 0.2 cm) and FTY720-treated groups (5.9 ± 0.1 cm) on day 14 p.i. At necropsy, changes in distal colonic weight were assessed as an indirect measurement of epithelial hyperplasia, mucosal inflammation, and hyperemia, all of which are common features of *C. rodentium*

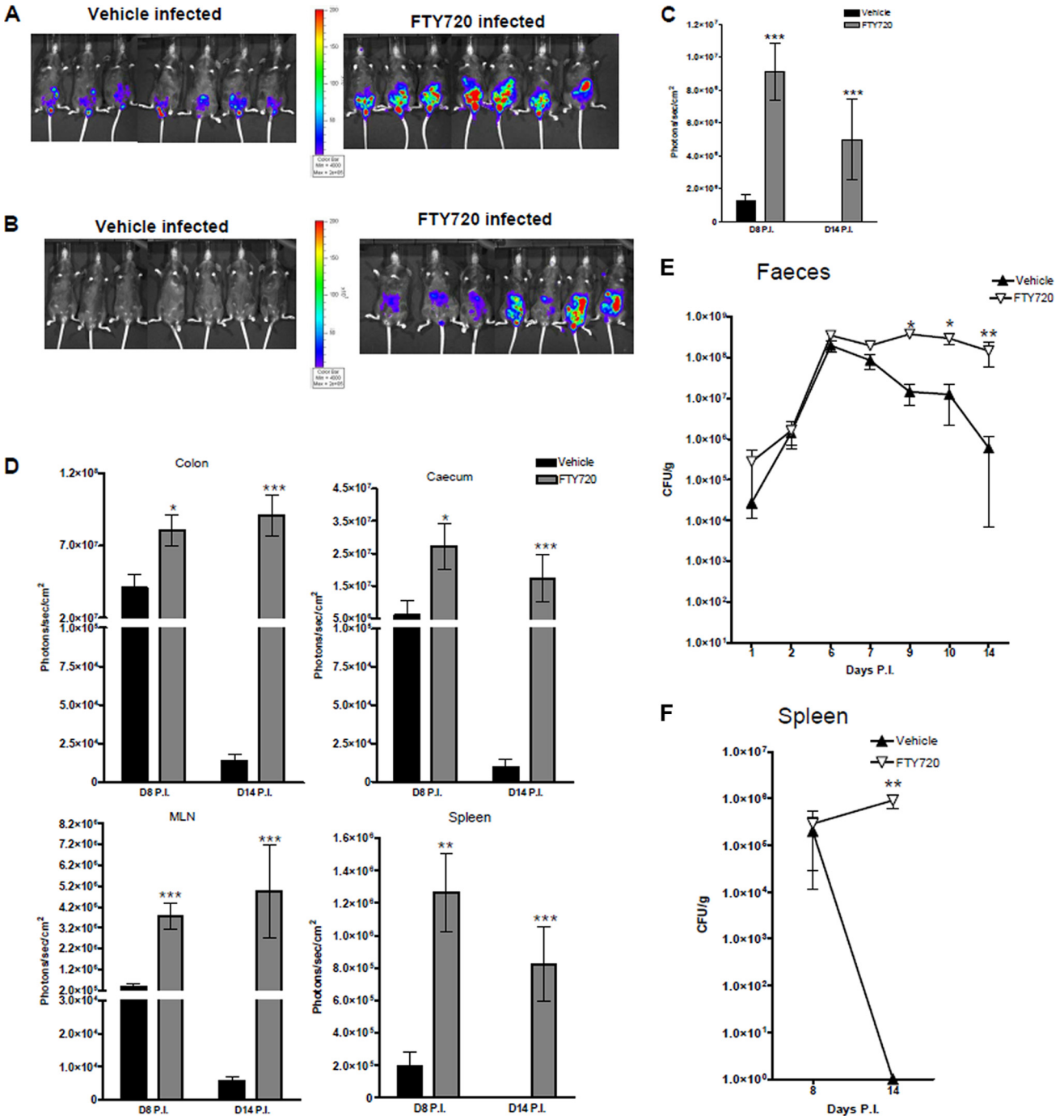

FIG 2 FTY720 treatment impairs clearance of *C. rodentium* infection. Shown is whole-body bioluminescence imaging of vehicle-treated and FTY720-treated mice on days 8 (A) and 14 (B) p.i. with *C. rodentium*. Also shown are bioluminescent signals from the gastrointestinal region (*in vivo* whole-body imaging) (C) and from *ex vivo* organs, i.e., the colon, cecum, MLNs, and spleen (D). Data are expressed as the mean ± the SEM for 7 individual animals per group. The significance of differences was determined by the Mann-Whitney U test (***, $P < 0.001$; **, $P < 0.01$; *, $P < 0.05$). Colonization and clearance of *C. rodentium* in vehicle-treated and FTY720-treated mice as indicated by counts of viable bacteria (CFU/g) in the stool (E) and spleen (F). Samples were taken at different time points for 14 days p.i. Data are expressed as the mean of 7 to 14 individual mice ± the SEM. The significance of differences was determined by the Kruskal-Wallis test followed by Dunn's multiple-comparison test (**, $P < 0.01$; *, $P < 0.05$).

infection. Animals infected with *C. rodentium* had significantly heavier distal colons than their noninfected counterparts at both of the time points analyzed, i.e., day 8 ($P < 0.05$) and day 14 p.i. ($P < 0.001$) (Fig. 3A). Moreover, no differences in distal colonic weights were observed between the vehicle-treated and FTY720-treated, noninfected controls (see Fig. S1B in the supplemental material). In contrast, *C. rodentium*-infected mice that received FTY720 had heavier distal colons than those treated with the ve-

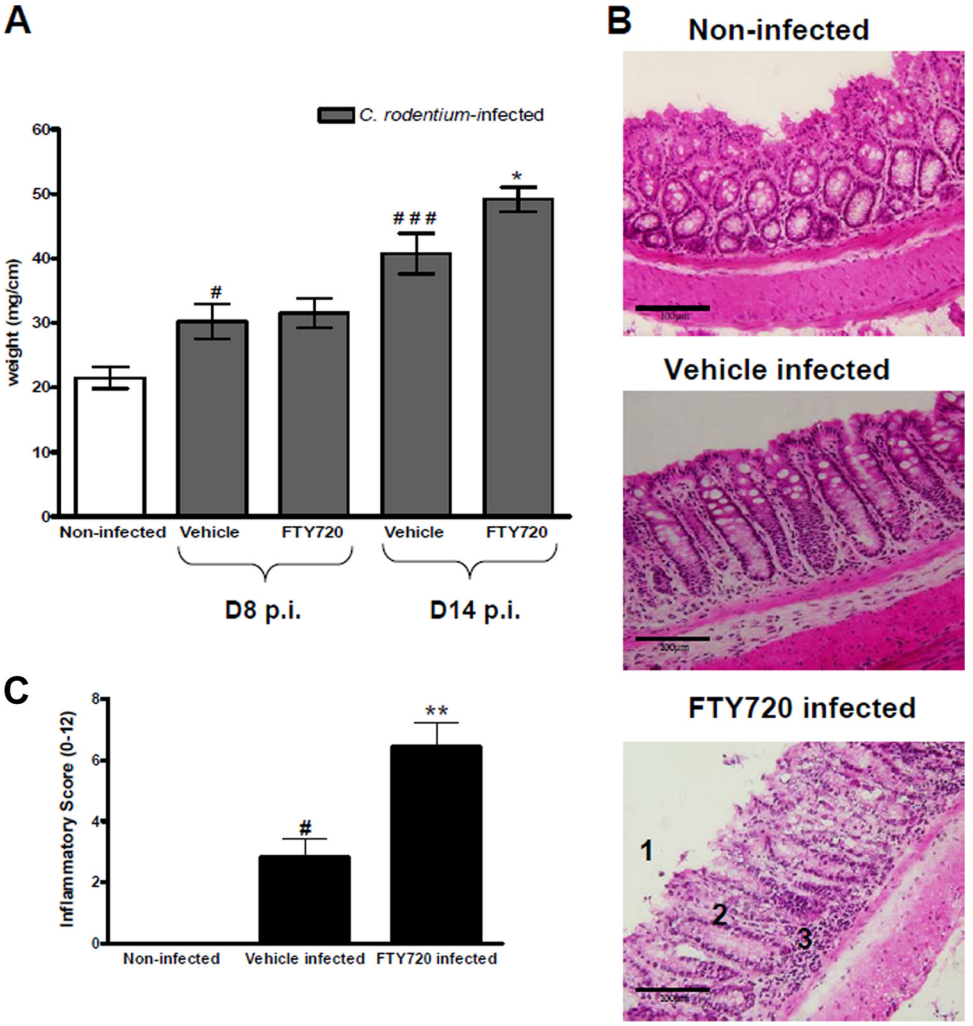

FIG 3 FTY720 treatment exacerbates colonic pathology during *C. rodentium* infection. (A) Differences in distal colon weight at days 8 (D8) and 14 (D14) p.i. The data represent the mean of 4 to 7 individual mice ± the SEM. The significance of differences between groups was determined by one-way analysis of variance, followed by Bonferroni's multiple-comparison test (#, $P < 0.05$ [noninfected versus vehicle on day 8]; # # #, $P < 0.001$ [noninfected versus vehicle on day 14]; *, $P < 0.05$ [vehicle versus FTY720]). (B) Representative histology tissue sections of distal colon segments on day 14 p.i. showing epithelial shedding (1), crypt elongation and goblet cell depletion (2), and mucosal thickening (3). Images are representative of 3 or 4 individual animals per group. Original magnification, ×40. Scale bars, 100 μm. (C) Mean inflammatory scores of vehicle- or FTY720-treated mice on day 14 p.i. determined by histological analysis of distal colonic sections (#, $P < 0.05$ [noninfected versus vehicle treated, infected]; **, $P < 0.01$ [vehicle treated versus FTY720 treated, infected]; $n = 3$ or 4 mice per group).

hicle on day 14 p.i., suggesting increased inflammation. This observation was supported by histological analysis of the distal colons, which revealed significantly increased inflammatory scores, i.e., greater mucosal thickening, epithelial cell hyperplasia, and goblet cell depletion, in the infected, FTY720-treated mice than in the infected, vehicle-treated controls (Fig. 3B and C). Although signs of inflammation and tissue damage were evident in the vehicle-treated colons, in contrast to the noninfected colons at day 14 p.i., it was much less severe and resolution and epithelial healing appeared to be taking place (Fig. 3B).

FTY720 alters the composition of immune cell populations infiltrating the colon during *C. rodentium* infection. To determine the effect of FTY720 on the composition and distribution of immune cell populations in the colon during *C. rodentium* infection, frozen colonic sections were fluorescently stained and analyzed for the numbers of $CD3^+$ T cells, $CD19^+$ B cells, $CD11c^+$ DCs, $F4/80^+$ macrophages, and $Ly6G^+$ neutrophils. A marked increase in the numbers of T cells ($P < 0.001$), B cells ($P < 0.05$), DCs ($P < 0.001$), macrophages ($P < 0.001$), and neutrophils ($P < 0.01$) was observed within the distal colons of the vehicle-treated animals compared to those of noninfected controls on day 14 p.i. (Fig. 4A and B). In comparison to those of the vehicle-treated animals, T and B lymphocytes ($P < 0.01$, $P < 0.001$), DCs ($P < 0.01$) and macrophages ($P < 0.001$) were significantly decreased in the distal colons of FTY720-treated animals at this time point (Fig. 4A and B). However, the numbers of neutrophils were significantly increased ($P < 0.05$) in these mice (Fig. 4A and B).

FTY720 treatment downregulates genes associated with the mucosal immune response to *C. rodentium*. To assess the effect of FTY720 treatment on the expression of innate and adaptive immunomodulatory genes during *C. rodentium* infection, we isolated distal colonic RNA and evaluated mRNA expression by real-time qPCR. In the distal colons of *C. rodentium*-infected animals that received the vehicle, the expression levels of innate immune

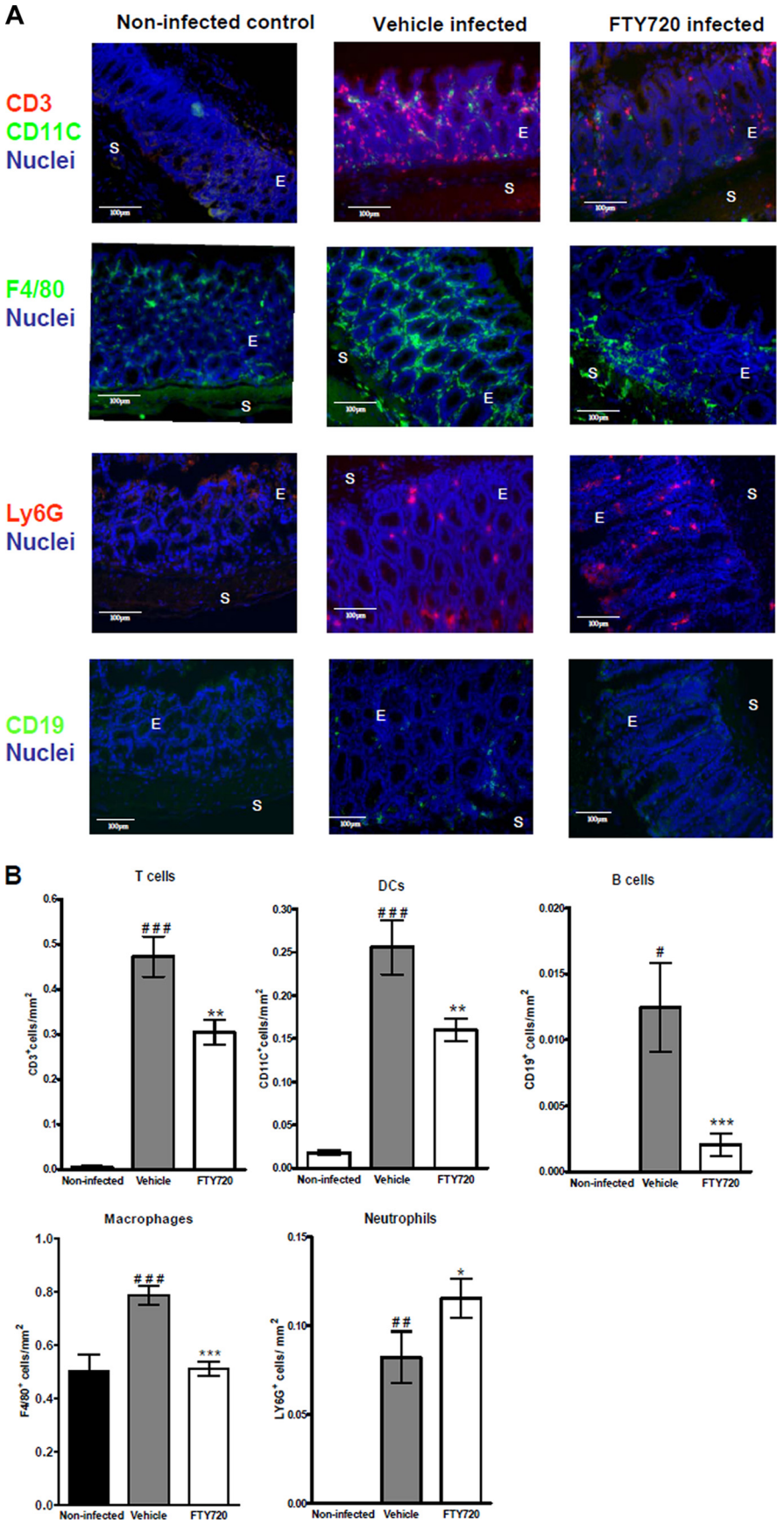
A
Non-infected control
Vehicle infected
FTY720 infected
CD3
CD11C
Nuclei
F4/80
Nuclei
Ly6G
Nuclei
CD19
Nuclei
S
E
B
T cells
DCs
B cells
Macrophages
Neutrophils
CD3+cells/mm2
CD11C+cells/mm2
CD19+cells/mm2
F4/80+cells/mm2
LY6G+cells/mm2
Non-infected
Vehicle
FTY720

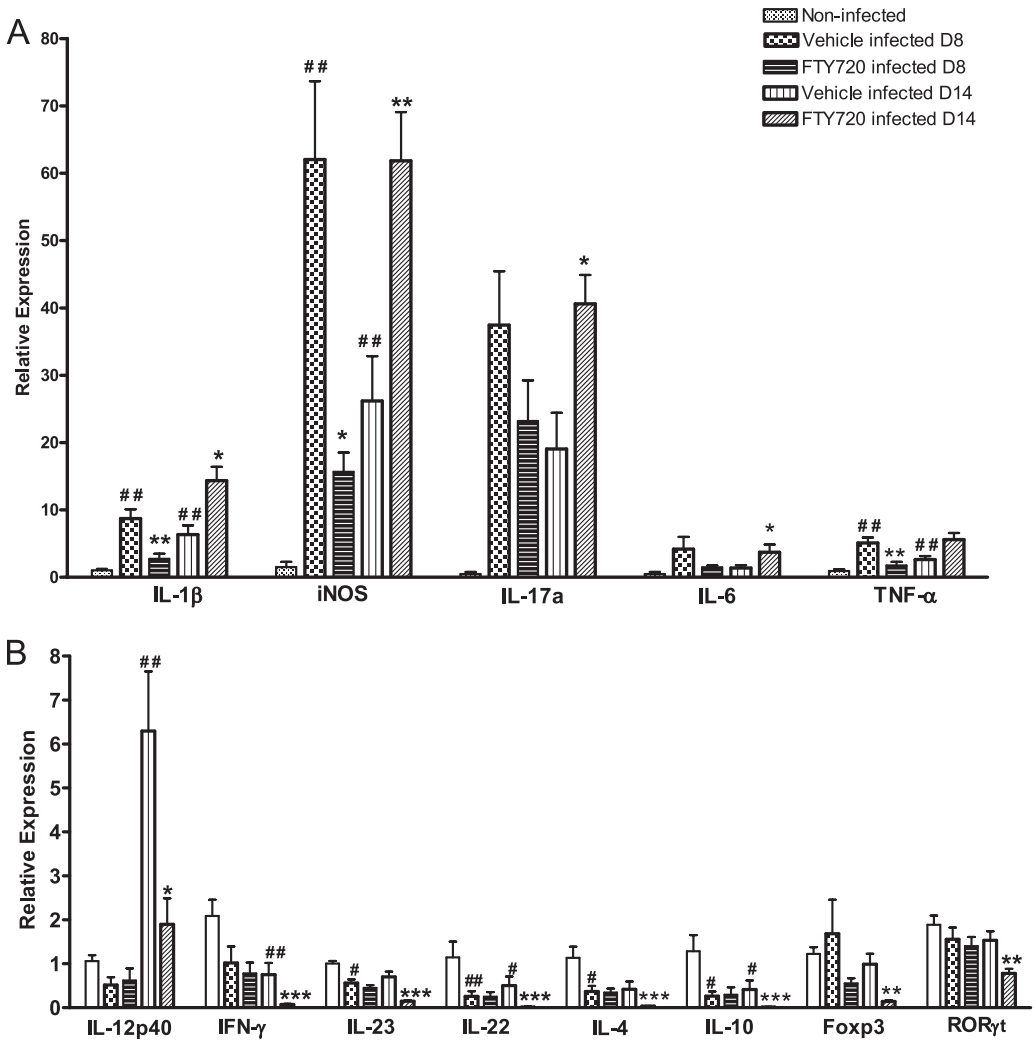

FIG 5 FTY720 impairs the mucosal immune response to *C. rodentium* infection. Distal colon mRNA extracts were analyzed for innate immune gene expression (A) and adaptive immune gene expression (B) on days 8 (D8) and 14 (D14) p.i. The $2^{-\Delta\Delta CT}$ method was used to calculate relative changes in gene expression compared with that in the noninfected (control) group. Expression was determined as *n*-fold induction compared with the β-actin housekeeper. Bars represent the mean of 4 to 6 individual mice ± the SEM. The significance of differences was determined by Mann-Whitney U test (# #, $P < 0.01$; #, $P < 0.05$ [noninfected control versus vehicle treated, infected]; ***, $P < 0.001$; **, $P < 0.01$; *, $P < 0.05$ [vehicle treated, infected versus FTY720 treated, infected]).

genes, such as those for the proinflammatory mediators IL-1β, iNOS, and TNF-α, were significantly upregulated compared to those of noninfected controls at day 8 p.i. This upregulation was significantly lower in FTY720-treated animals than in the vehicle-treated mice (Fig. 5A). In contrast, on day 14 p.i., the expression of these mediators, together with IL-17a and IL-6, was significantly upregulated in the drug-treated animals compared to that in the vehicle-treated controls at this time point (Fig. 5A). Similarly, TNF-α was also increased in these mice at this time point ($P = 0.053$). Genes associated with an adaptive T cell response, such as those for IL-23, IL-22, IL-4, and IL-10, were significantly decreased in infected, vehicle-treated mice compared to those in noninfected controls at day 8 p.i. This downregulation was not significantly affected by FTY720 treatment at this time point (Fig. 5B). In contrast, expression of the gene for the Th1 cytokine IL-12p40 was significantly upregulated in infected, vehicle-treated mice compared to that in noninfected controls at day 14 p.i. However, a significant upregulation of the other T cell-associated cytokine genes was not detected in infected, vehicle-treated mice compared to that in noninfected mice at this time point. Never-

FIG 4 FTY720 alters the composition of immune cell populations in the colon during infection. Tissue sections obtained from 4 individual mice on day 14 p.i. were analyzed by fluorescence microscopy. (A) Serial frozen sections (6 μm) were fixed in acetone-ethanol and stained for $CD11c^+$, $F4/80^+$, and $CD19^+$ cells (green) and costained for $CD3^+$ cells, $LY6G^+$ cells (red), and nuclei (blue). A representative picture for each group is shown. Original magnification, ×40. Scale bars, 100 μm. E indicates epithelium, and S shows submucosa. (B) Quantitation of cells/mm^2 of tissue. Bars represent the mean ± the SEM of the total number of positive cells/mm^2. Values are based on 3 or 4 individual mice, measuring 7 to 10 fields at ×40 magnification of distal colons. The significance of differences between groups was determined by one-way analysis of variance, followed by Bonferroni's multiple-comparison test (#, $P < 0.05$; # #, $P < 0.01$; # # #, $P < 0.001$ [noninfected versus vehicle treated, infected]; *, $P < 0.05$; **, $P < 0.01$; ***, $P < 0.001$ [vehicle treated, infected versus FTY720 treated, infected]).

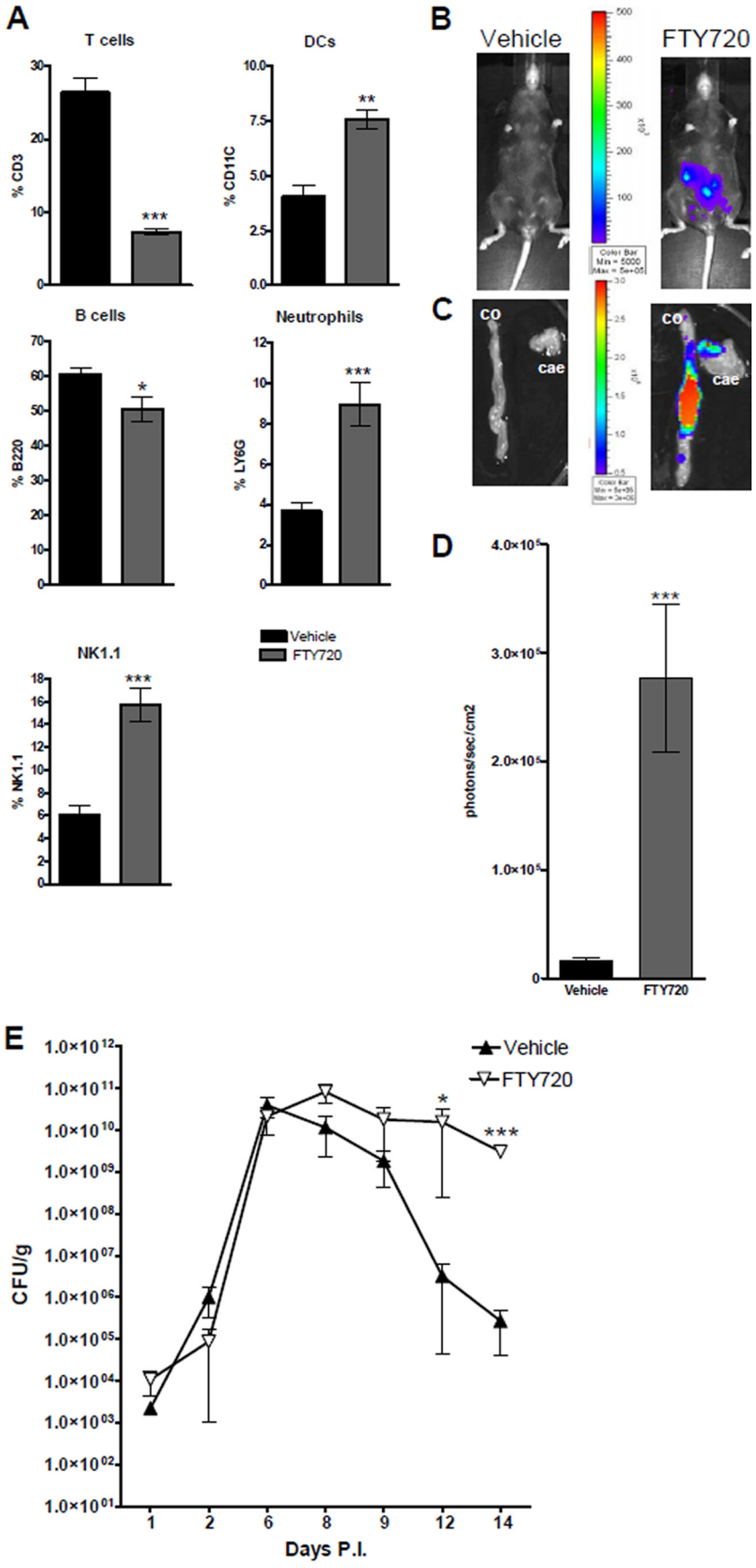
A
T cells
% CD3
***
DCs
% CD11C
**
B cells
% B220
*
Neutrophils
% LY6G
***
Vehicle
FTY720
NK1.1
% NK1.1
***
B
Vehicle
FTY720
C
co
cae
co
cae
D
photons/sec/cm2
4.0×10⁵
3.0×10⁵
2.0×10⁵
1.0×10⁵
0
***
Vehicle
FTY720
E
CFU/g
Vehicle
FTY720
*
***
Days P.I.
1
2
6
8
9
12
14

theless, colonic expression of IL-12p40, IFN-γ, IL-22, IL-10, IL-4, the Treg transcription factor Foxp3, and the Th17 inducers RORγt and IL-23 was significantly decreased in infected, FTY720-treated compared to that in infected, vehicle-treated mice at day 14 p.i. (Fig. 5B). No significant changes in the expression of Tbet or REGIIIγ were observed in infected, FTY720-treated versus that in vehicle-treated animals. Real-time qPCR analysis of colonic gene expression in vehicle-treated and FTY720-treated, noninfected controls was also carried out, but no significant changes were observed (data not shown).

Termination of FTY720 treatment at early time points p.i. had minimal effects on peripheral blood lymphopenia or pathogen clearance. To determine what effect termination of FTY720 dosing has during early *C. rodentium* infection, mice were administered the vehicle or the S1P analogue daily for 6 days prior to *C. rodentium* infection and 2 days after infection. On day 14 p.i., blood leukocyte populations, colonization, and clinical and macroscopic markers of infection were determined. In the infected mice that had been treated with FTY720, peripheral blood lymphopenia was maintained, as were the enhanced numbers of DCs (Fig. 6A). Unlike with continuous dosing p.i., levels of peripheral granulocytes and NK cells in blood were increased compared to those in infected, vehicle-treated mice (Fig. 6A). Whole-body bioluminescence imaging revealed that the FTY720-treated mice were still heavily colonized by day 14 p.i. (Fig. 6B) and had greater signals from their colons ($P < 0.001$, Fig. 6C and D), ceca ($P < 0.001$, Fig. 6C; see Fig. S3 in the supplemental material), MLNs, and spleens ($P < 0.001$, see Fig. S3 in the supplemental material). These data were supported by fecal CFU counts (Fig. 6E). However, no differences in disease activity or distal colon weight were evident between the infected, vehicle-treated mice and those that had received FTY20.

DISCUSSION

The results of this study show that FTY720 delayed the clearance of the murine enteric pathogen *C. rodentium*. This was most likely a result of FTY720-mediated peripheral lymphopenia and T cell entrapment within the LNs, resulting in impairment of the adaptive immune response within the colon. Additionally, the colonic innate immune response was impaired and there was increased colon pathology and bacterial dissemination.

Our data show that FTY720 induced peripheral blood lymphopenia pre- and postinfection and T cell entrapment within the MLNs, which is consistent with previous reports (1, 3). Data from bioluminescence imaging of whole bodies and organs combined with counts of viable bacteria in the stool and spleen revealed that FTY720-treated mice were highly susceptible to colonic and systemic infection with *C. rodentium*. In addition to an increased bacterial burden, more extensive pathogen distribution, and impaired bacterial clearance, these mice exhibited higher disease activity at peak infection and greater colonic pathology at day 14 p.i. These findings are in contrast to what has been previously demonstrated in experimental models of colitis reflecting inflammatory bowel disease (11, 12, 14, 18, 36). In these instances, FTY720 had a therapeutic effect on disease by blunting immunity. In the present study, FTY720 blocked lymphocyte migration to the *C. rodentium*-infected intestine. Notably, FTY720-treated mice had reduced numbers of colonic T cells, DCs, B cells, and macrophages but increased numbers of neutrophils at day 14 p.i. than vehicle-treated, infected controls. These results are reminiscent of those observed in T and B cell-deficient RAG1 knockout (KO) mice (45). In fact, *C. rodentium* infection of these mice also leads to a predominantly granulocytic colonic infiltrate and an enhanced bacterial presence in their peripheral organs, as well as their colons (34, 45, 54).

Neutrophils are important in the early innate immune response to infection with bacteria such as *C. rodentium*, preventing dissemination and controlling the bacterial load (32, 50). However, during chronic inflammatory disease, they can contribute to host tissue pathology (26, 41, 49). In the present study, an increased neutrophil presence in the infected colons of FTY720-treated mice at day 14 p.i. was accompanied by enhanced severity of colonic inflammation. Interestingly, this increased neutrophil influx was also associated with upregulated expression of the genes for the innate immune response-related cytokines IL-1β, iNOS, IL-17a, IL-6, and TNF-α at day 14 p.i. In agreement with previous reports, we found that the expression of the genes for these innate immune cytokines was higher in infected, vehicle-treated mice than in noninfected controls at peak infection (22, 48). These cytokines play a significant role in host defense and clearance of *C. rodentium* early during infection (13, 20, 25, 53). In the present study, it is possible that the innate immune response attempted to compensate for the blunted adaptive response in the infected, FTY720-treated colons at day 14 p.i (32). Another possibility is that FTY720 impaired the innate immune response at peak infection, a notion supported by the downregulation of these cytokines in the FTY720-treated colons compared to those in vehicle-treated mice at day 8. The fact that the delayed innate response is unsuccessful at day 14 p.i. does not preclude the possibility that, at later time points, the heightened neutrophilic response may eventually promote the clearance of *C. rodentium*. However, it should be noted that long-term-infected RAG1 KO mice (up to day 60 p.i.) also fail to clear their *C. rodentium* infection (54).

The reduction in T cells, DCs, and macrophages in the colons of the infected, FTY720-treated mice at day 14 was in accordance

FIG 6 Termination of FTY720 treatment postinfection had minimal effects on peripheral blood lymphopenia or pathogen colonization. (A) Percentages of leukocyte populations in blood. Mice were treated with FTY720 or the vehicle for 6 days prior to *C. rodentium* infection and 2 days p.i. Leukocytes were isolated from the blood of vehicle-treated and FTY720-treated, *C. rodentium*-infected animals on day 14 p.i. and stained with a fluorochrome-labeled MAb. They were analyzed by flow cytometry, in which 10,000 to 20,000 events were recorded. The data represent the mean percentages of $CD3^+$ (T cells), $CD11c^+$ (DCs), $B220^+$ (B cells), and $Ly6G^+$ (neutrophils) cells at two time points during *C. rodentium* infection. The significance of differences between vehicle-treated (control) animals and FTY720-treated animals was determined by the Mann-Whitney U test (***, $P < 0.001$; **, $P < 0.01$;*, $P < 0.05$; $n = 6$ to 8 individual mice). Effect of FTY720 on the pathogen burden and clearance of *C. rodentium* infection. Representative images of whole-body (B) and *ex vivo* colon (co) and cecum (cae) (C) bioluminescence of vehicle-treated and FTY720-treated mice at day 14 p.i. are shown. (D) Bioluminescent signal from the colon. Data are expressed as the mean ± the SEM of 6 to 8 individual mice per group. The significance of differences was determined by the Mann-Whitney U test (***, $P < 0.001$). (E) Colonization and clearance of *C. rodentium* in vehicle-treated and FTY720-treated mice as indicated by counts of viable bacteria (CFU/g) in stool samples. Samples were taken at different time points for 14 days p.i. Data are expressed as the mean of 6 to 8 individual mice ± the SEM. The significance of differences was determined by the Kruskal-Wallis test, followed by Dunn's multiple-comparison test (**, $P < 0.01$; *, $P < 0.05$).

with the decreased colonic expression of IL-12p40, IFN-γ, IL-23, IL-22, IL-4, IL-10, Foxp3, and RORγt mRNAs in these mice at this time point. *C. rodentium* infection is associated with a highly polarized Th1 host immune response (22), and IL-12p40 is essential for adequate clearance of the pathogen from the gut (46). The cytokines IFN-γ (44), IL-22, and IL-23 (57) also play important roles in the host defense against *C. rodentium*, and their downregulation in FTY720-treated animals may have contributed to the increased bacterial burden and dissemination. However, with the exception of IL-12p40, we did not see infection-specific induction of the other T cell-associated cytokines analyzed at day 8 or day 14 p.i. This may be due to the kinetics of the immune response in the model and the time points analyzed in this study.

Importantly, we also demonstrated that termination of FTY720 treatment early after infection had little or no effect on pathogen clearance or immune profiles. This finding highlights the fact that, in a clinical setting, even with early diagnosis of infection, patients might still be highly susceptible to disease for at least 2 weeks or longer after the termination of drug treatment.

To our knowledge, this is the first study that has investigated the effect of FTY720 treatment on a model of gastrointestinal infection. Previous studies using virus or antigen-specific virus inducers have suggested a risk of impairment of immune responses by FTY720 (23, 42). Apart from the two fatalities reported, clinical studies of MS patients have found no other major complications regarding the risk of infection, except for a higher incidence of lower respiratory tract and lung infections in patients treated with FTY720 than in placebo-treated patients (8, 28). However, based on the present study, vigilance for bacterial infections should be maintained, especially in patients with other autoimmune or intestinal inflammatory conditions, where FTY720 may be considered for future therapeutic treatment. Further studies examining the effects of FTY720 treatment on antigen-specific immune responses upon exposure to a range of viral and bacterial infections are therefore required.

ACKNOWLEDGMENTS

The Alimentary Pharmabiotic Centre is a research center funded by Science Foundation Ireland (SFI).

We and our work are supported by SFI grants 02/CE/B124 and 07/CE/B1368.

REFERENCES

1. **Brinkmann V, et al.** 2010. Fingolimod (FTY720): discovery and development of an oral drug to treat multiple sclerosis. Nat. Rev. Drug Discov. **9**:883–897.
2. **Brinkmann V, et al.** 2002. The immune modulator FTY720 targets sphingosine 1-phosphate receptors. J. Biol. Chem. **277**:21453–21457.
3. **Brinkmann V, Lynch KR.** 2002. FTY720: targeting G-protein-coupled receptors for sphingosine 1-phosphate in transplantation and autoimmunity. Curr. Opin. Immunol. **14**:569–575.
4. **Budde K, et al.** 2002. First human trial of FTY720, a novel immunomodulator, in stable renal transplant patients. J. Am. Soc. Nephrol. **13**:1073–1083.
5. **Chi H, Flavell RA.** 2005. Cutting edge: regulation of T cell trafficking and primary immune responses by sphingosine 1-phosphate receptor 1. J. Immunol. **174**:2485–2488.
6. **Chiba K, Matsuyuki H, Maeda Y, Sugahara K.** 2006. Role of sphingosine 1-phosphate receptor type 1 in lymphocyte egress from secondary lymphoid tissues and thymus. Cell. Mol. Immunol. **3**:11–19.
7. **Cohen JA, et al.** 2010. Oral fingolimod or intramuscular interferon for relapsing multiple sclerosis. N. Engl. J. Med. **362**:402–415.
8. **Collins W, et al.** 2010. Long-term safety of oral fingolimod (FTY720) in relapsing multiple sclerosis: integrated analyses of phase 2 and 3 studies. Mult. Scler. **16**:S295.
9. **Contag CH, et al.** 1995. Photonic detection of bacterial pathogens in living hosts. Mol. Microbiol. **18**:593–603.
10. **Costa GL, et al.** 2001. Adoptive immunotherapy of experimental autoimmune encephalomyelitis via T cell delivery of the IL-12 p40 subunit. J. Immunol. **167**:2379–2387.
11. **Daniel C, et al.** 2007. FTY720 ameliorates Th1-mediated colitis in mice by directly affecting the functional activity of $CD4^+$ $CD25^+$ regulatory T cells. J. Immunol. **178**:2458–2468.
12. **Daniel C, et al.** 2007. FTY720 ameliorates oxazolone colitis in mice by directly affecting T helper type 2 functions. Mol. Immunol. **44**:3305–3316.
13. **Dann SM, et al.** 2008. IL-6-dependent mucosal protection prevents establishment of a microbial niche for attaching/effacing lesion-forming enteric bacterial pathogens. J. Immunol. **180**:6816–6826.
14. **Deguchi Y, et al.** 2006. The S1P receptor modulator FTY720 prevents the development of experimental colitis in mice. Oncol. Rep. **16**:699–703.
15. **Edinger M, Hoffmann P, Contag CH, Negrin RS.** 2003. Evaluation of effector cell fate and function by in vivo bioluminescence imaging. Methods **31**:172–179.
16. **Eigenbrod S, Derwand R, Jakl V, Endres S, Eigler A.** 2006. Sphingosine kinase and sphingosine-1-phosphate regulate migration, endocytosis and apoptosis of dendritic cells. Immunol. Invest. **35**:149–165.
17. **Francis KP, et al.** 2001. Visualizing pneumococcal infections in the lungs of live mice using bioluminescent *Streptococcus pneumoniae* transformed with a novel gram-positive *lux* transposon. Infect. Immun. **69**:3350–3358.
18. **Fujii R, et al.** 2006. FTY720 suppresses $CD4^+$ $CD44^{high}$ $CD62L^-$ effector memory T cell-mediated colitis. Am. J. Physiol. Gastrointest. Liver Physiol. **291**:G267–G274.
19. **Garber K.** 2008. Infections cast cloud over Novartis' MS therapy. Nat. Biotechnol. **26**:844–845.
20. **Gobert AP, et al.** 2004. Protective role of arginase in a mouse model of colitis. J. Immunol. **173**:2109–2117.
21. **Gräler MH, Goetzl EJ.** 2004. The immunosuppressant FTY720 downregulates sphingosine 1-phosphate G-protein-coupled receptors. FASEB J. **18**:551–553.
22. **Higgins LM, Frankel G, Douce G, Dougan G, MacDonald TT.** 1999. *Citrobacter rodentium* infection in mice elicits a mucosal Th1 cytokine response and lesions similar to those in murine inflammatory bowel disease. Infect. Immun. **67**:3031–3039.
23. **Horga A, Castillo J, Montalban X.** 2010. Fingolimod for relapsing multiple sclerosis: an update. Expert Opin. Pharmacother. **11**:1183–1196.
24. **Hoshino Y, et al.** 1996. FTY720, a novel immunosuppressant possessing unique mechanisms. II. Long-term graft survival induction in rat heterotopic cardiac allografts and synergistic effect in combination with cyclosporine A. Transplant. Proc. **28**:1060–1061.
25. **Ishigame H, et al.** 2009. Differential roles of interleukin-17A and -17F in host defense against mucoepithelial bacterial infection and allergic responses. Immunity **30**:108–119.
26. **Ito R, et al.** 2008. Involvement of IL-17A in the pathogenesis of DSS-induced colitis in mice. Biochem. Biophys. Res. Commun. **377**:12–16.
27. **Kappos L, et al.** 2006. Oral fingolimod (FTY720) for relapsing multiple sclerosis. N. Engl. J. Med. **355**:1124–1140.
28. **Kappos L, et al.** 2010. A placebo-controlled trial of oral fingolimod in relapsing multiple sclerosis. N. Engl. J. Med. **362**:387–401.
29. **Kenny B, et al.** 1997. Enteropathogenic E. coli (EPEC) transfers its receptor for intimate adherence into mammalian cells. Cell **91**:511–520.
30. **Kersh EN, et al.** 2009. Evaluation of the lymphocyte trafficking drug FTY720 in SHIVSF162P3-infected rhesus macaques. J. Antimicrob. Chemother. **63**:758–762.
31. **Lan YY, et al.** 2005. The sphingosine-1-phosphate receptor agonist FTY720 modulates dendritic cell trafficking in vivo. Am. J. Transplant. **5**:2649–2659.
32. **Lebeis SL, Bommarius B, Parkos CA, Sherman MA, Kalman D.** 2007. TLR signaling mediated by MyD88 is required for a protective innate immune response by neutrophils to Citrobacter rodentium. J. Immunol. **179**:566–577.
33. **Livak KJ, Schmittgen TD.** 2001. Analysis of relative gene expression data using real-time quantitative PCR and the 2(−Delta Delta C(T)) Method. Methods **25**:402–408.
34. **Maaser C, et al.** 2004. Clearance of *Citrobacter rodentium* requires B cells but not secretory immunoglobulin A (IgA) or IgM antibodies. Infect. Immun. **72**:3315–3324.

35. **Mehling M, Johnson TA, Antel J, Kappos L, Bar-Or A.** 2011. Clinical immunology of the sphingosine 1-phosphate receptor modulator fingolimod (FTY720) in multiple sclerosis. Neurology **76**(Suppl 3):S20–S27.
36. **Mizushima T, et al.** 2004. Therapeutic effects of a new lymphocyte homing reagent FTY720 in interleukin-10 gene-deficient mice with colitis. Inflamm. Bowel Dis. **10**:182–192.
37. **Mundy R, MacDonald TT, Dougan G, Frankel G, Wiles S.** 2005. Citrobacter rodentium of mice and man. Cell. Microbiol. **7**:1697–1706.
38. **Murphy CT, et al.** 2010. Use of bioluminescence imaging to track neutrophil migration and its inhibition in experimental colitis. Clin. Exp. Immunol. **162**:188–196.
39. **Murphy CT, et al.** 2010. Technical advance: function and efficacy of an {alpha}4-integrin antagonist using bioluminescence imaging to detect leukocyte trafficking in murine experimental colitis. J. Leukoc. Biol. **88**: 1271–1278.
40. **Rocchetta HL, et al.** 2001. Validation of a noninvasive, real-time imaging technology using bioluminescent *Escherichia coli* in the neutropenic mouse thigh model of infection. Antimicrob. Agents Chemother. **45**:129–137.
41. **Sartor RB.** 1994. Cytokines in intestinal inflammation: pathophysiological and clinical considerations. Gastroenterology **106**:533–539.
42. **Schmouder R, Boulton C, Wang N, David OJ.** 2010. Effects of fingolimod on antibody response following steady-state dosing in healthy volunteers: a 4-week randomised, placebo-controlled study (P412). Mult. Scler **16**(Suppl 10):S135.
43. **Sheikh AY, et al.** 2007. Molecular imaging of bone marrow mononuclear cell homing and engraftment in ischemic myocardium. Stem Cells **25**: 2677–2684.
44. **Shiomi H, et al.** 2010. Gamma interferon produced by antigen-specific $CD4^+$ T cells regulates the mucosal immune responses to *Citrobacter rodentium* infection. Infect. Immun. **78**:2653–2666.
45. **Simmons CP, et al.** 2003. Central role for B lymphocytes and $CD4^+$ T cells in immunity to infection by the attaching and effacing pathogen *Citrobacter rodentium*. Infect. Immun. **71**:5077–5086.
46. **Simmons CP, et al.** 2002. Impaired resistance and enhanced pathology during infection with a noninvasive, attaching-effacing enteric bacterial pathogen, Citrobacter rodentium, in mice lacking IL-12 or IFN-gamma. J. Immunol. **168**:1804–1812.
47. **Sinha RK, Park C, Hwang IY, Davis MD, Kehrl JH.** 2009. B lymphocytes exit lymph nodes through cortical lymphatic sinusoids by a mechanism independent of sphingosine-1-phosphate-mediated chemotaxis. Immunity **30**:434–446.
48. **Smith AD, Botero S, Shea-Donohue T, Urban JF, Jr.** 2011. The pathogenicity of an enteric *Citrobacter rodentium* infection is enhanced by deficiencies in the antioxidants selenium and vitamin E. Infect. Immun. **79**: 1471–1478.
49. **Southey A, et al.** 1997. Pathophysiological role of nitric oxide in rat experimental colitis. Int. J. Immunopharmacol. **19**:669–676.
50. **Spehlmann ME, et al.** 2009. CXCR2-dependent mucosal neutrophil influx protects against colitis-associated diarrhea caused by an attaching/effacing lesion-forming bacterial pathogen. J. Immunol. **183**:3332–3343.
51. **Sweeney TJ, et al.** 1999. Visualizing the kinetics of tumor-cell clearance in living animals. Proc. Natl. Acad. Sci. U. S. A. **96**:12044–12049.
52. **Thangada S, et al.** 2010. Cell-surface residence of sphingosine 1-phosphate receptor 1 on lymphocytes determines lymphocyte egress kinetics. J. Exp. Med. **207**:1475–1483.
53. **Vallance BA, et al.** 2002. Modulation of inducible nitric oxide synthase expression by the attaching and effacing bacterial pathogen *Citrobacter rodentium* in infected mice. Infect. Immun. **70**:6424–6435.
54. **Vallance BA, Deng W, Knodler LA, Finlay BB.** 2002. Mice lacking T and B lymphocytes develop transient colitis and crypt hyperplasia yet suffer impaired bacterial clearance during *Citrobacter rodentium* infection. Infect. Immun. **70**:2070–2081.
55. **Wiles S, et al.** 2004. Organ specificity, colonization and clearance dynamics in vivo following oral challenges with the murine pathogen Citrobacter rodentium. Cell. Microbiol. **6**:963–972.
56. **Wolf AM, et al.** 2009. The sphingosine 1-phosphate receptor agonist FTY720 potently inhibits regulatory T cell proliferation in vitro and in vivo. J. Immunol. **183**:3751–3760.
57. **Zheng Y, et al.** 2008. Interleukin-22 mediates early host defense against attaching and effacing bacterial pathogens. Nat. Med. **14**:282–289.
58. **Zhi L, et al.** 2011. FTY720 blocks egress of T cells in part by abrogation of their adhesion on the lymph node sinus. J. Immunol. **187**:2244–2251.